Upper critical fields in granular superconductors

G. Deutscher, O. Entin-Wohlman, and Y. Shapira
Department of Physics and Astronomy, Tel Aviv University, Tel Aviv, Israel
(Received 6 December 1979)

We have measured the upper critical field in granular Al-Ge samples, as a function of temperature and for different metal concentrations. For small metal concentrations, we find that the upper critical field of the sample is that of the isolated grains at all temperatures. For high metal concentrations, the upper critical field is that of a bulk dirty superconductor. For intermediate metal concentrations, one observes a crossover from the bulk type-II behavior at high temperatures to the isolated grain behavior at low temperatures, with an upturn of the critical field at the crossover temperature. We present a Landau-Ginzburg model for the critical fields in a granular system and show that it explains the experimental data.

I. INTRODUCTION

The upper critical fields of granular superconductors were first measured by Abeles *et al.*[1] and Cohen and Abeles[2] who interpreted their results with a model treating the granular superconductor as a dirty type-II material. Latter data obtained on higher resistivity samples by Deutscher and Dodds[3] showed a behavior similar to that of isolated layers or grains. From the available data[1–4] it therefore appears that three regimes can be distinguished in the behavior of H_{c2}. (a) At high values of the resistivity ρ_n, the measured critical field is that of the isolated grains (weak-coupling regime). (b) At low values of ρ_n the grains are strongly coupled and the system can be described as a dirty bulk superconductor. (c) At intermediate values of ρ_n the temperature dependence of H_{c2} exhibits an upturn point at a temperature below which the grains become weakly coupled. The behavior of H_{c2}, as a function of temperature and grain size, can be complicated by paramagnetic effects in the isolated grain limit (case a) or effects due to the small thickness of the specimen.

While the assumption[1,2,4] that the granular system can be considered as a dirty superconductor may be adequate when the grains are strongly coupled, it is certainly unsuitable for the description of weakly coupled or almost isolated grains. In the last case, one should consider clean superconducting grains separated by barriers, and it is conceivable to expect a type of "clean" behavior: This was pointed out in Refs. 3 and 5, where the results were interpreted qualitatively in terms of a layered superconducting system.

In this article we present a Landau-Ginzburg (LG) theory for H_{c2} of a granular system, together with H_{c2} measurements taken on granular Al embedded in a Ge matrix. This experimental system was chosen because the Al grains are fairly large (100–150 Å for the metal concentrations studied here), so that the isolated grains are not in the paramagnetic limit. Assuming that the coupling between the grains is through the Josephson interaction, we were able to extract from our theory expressions for H_{c2} in the different regimes described above and to fit them well with the experimental data. In case (a) (isolated grain limit) the theoretical H_{c2} gives the measured H_{c2} without any adjustable parameter. Moreover, it is observed that in this regime the value of H_{c2} depends only on the grain size, for different values of ρ_n. This is a novel result which proves that the measured H_{c2} is indeed that of an isolated grain. In case (b), the theoretical H_{c2} fits the experimental value up to a factor of 2. In the crossover region, our model describes well the qualitative behavior of H_{c2} as a function of the temperature, but the value of H_{c2} at the crossover point is off from that of the measured H_{c2}.

Sample preparation, measuring techniques and specimen characterization are detailed in Sec. II, and the experimental results are presented in Sec. III. The theoretical model is developed in Sec. IV. Section V contains an extensive comparison of the theorical results with the experimental data reported here and by other authors. Corrections due to the small thickness of the samples are presented, and the numerical differences between the theoretical and the measured results, as well as the question of observing an isolated grain's property through an electrical measurement are discussed.

II. EXPERIMENTAL DETAILS

Samples were prepared by a simultaneous evaporation of Al and Ge from two electron-beam guns, onto a glass substrate, in vacuum of 10^{-6} Torr. The total deposition rate was 40–50 Å/sec, and the thicknesses of the films were 1500–2000 Å. The

thickness was measured during deposition by two separate quartz crystal oscillators.

The substrate was mounted on a holder positioned along the line between the two guns. Because of this geometrical arrangement, the metal concentration varies along the substrate. Using a suitable mask, we could produce nine samples at the same evaporation, each sample being 2×8 mm^2. Calibration of the nine stations was done by an optical interferometer, and the metal concentration varied by 1–2% from sample to sample. This procedure allowed scanning of different metal concentrations, keeping the relative experimental error small. Contacts of 3000 Å thickness were evaporated after depositions, to which indium contacts were pressed.

Resistance measurements were taken by the conventional four-terminal technique, using currents of 1–100 μA. During the measurement, the samples were attached to a copper block and the temperature was monitored by a Ge thermometer. The parallel magnetic field was applied from a small superconducting magnet, immersed in the liquid He bath. The field was applied perpendicular to the measuring current.

The critical temperature and the critical field were defined as the point at which the resistance reached half its value. However, except for small changes in temperature scale, other choices for T_c made no difference.

Electron microscopy pictures were taken for about half of the measured samples. This was accomplished by mounting nine microscope grids coated with 300 Å of SiO along the glass substrate. In this way, the metal concentrations on the grids reflected those in the samples. Diffraction patterns, as well as microscope pictures with enlargement of 100 000 were studied for most grids. In some cases, bright field microscopy was found to be unsuitable, for reasons described in Ref. 6. In these cases dark-field microscopy was utilized.

III. RESULTS

Electron-microscopy pictures reveal that the samples consist of small grains separated by barriers. The diffraction patterns show and confirm (see Ref. 7), that these are polycrystalline Al grains, embedded in an amorphous Ge matrix. In each picture we have measured the grain size and constructed a histogram. Typical example is shown in Fig. 1. It was found that for low metal concentrations (~ 55–75%), the sizes of the grains roughly obey a normal distribution, with a standard deviation less than 15% of the mean value. At higher concentrations, the grain size is distributed over a broad range, but then, close to the pure metal limit, the grain size is not well defined in any case. In the range of concentrations studied here (60–88%), the grain size varies from ~ 100±10 Å

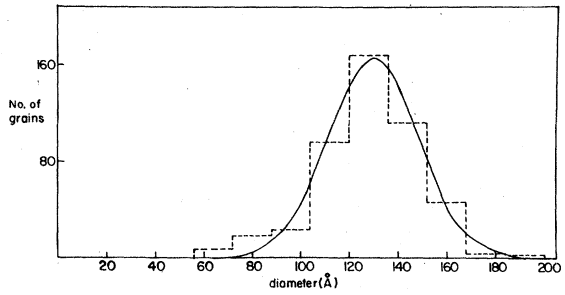

FIG. 1. Grain size distribution of sample 1 obtained by dark field electron microscopy with an enlargement of 100 000. The dashed line represents a histogram measured from the microscope pictures. The full line is a best fit normal distribution curve for the histogram. The standard deviation was found to be 20 Å.

to ~ 150±10 Å. Throughout the computations, we have chosen 100 and 150 Å to represent the grain size in the low- and high-concentration regimes, respectively.

In Table I we have listed the characteristics of the samples for which the $H_{c2}(T)$ data are depicted in Figs. 2 and 3. We have used the ratio ρ_n (300 K)/ρ_n (77 K), where ρ_n is the normal-state resistivity, to characterize the metallic or semiconductor nature of the samples, thus avoiding complications due to paraconductivity at 4.2 K. The curves of $H_{c2}(T)$ shown in Fig. 2 are typical for dirty Al films; decreasing the metal concentration by 2% from that of sample 1 in Fig. 2, caused a semiconducting behavior

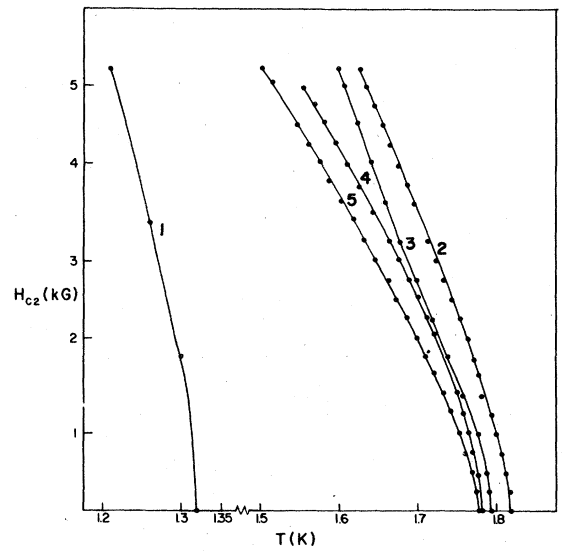

FIG. 2. H_{c2} vs temperature for dirty Al films with metal concentrations 64–74% (experimental).

TABLE I. Characteristics of samples for which $H_{c2}(T)$ data are presented in Figs. 2 and 3. d is the sample's thickness.

Sample	d (Å)	[metal] (%)	$\rho_{4.2\,K}$ ($\mu\Omega$cm)	$\rho_{300\,K}/\rho_{77\,K}$
1	2130	65.5	50 700	0.488
2	2170	67.5	16 000	0.600
3	2220	69.5	6 600	0.716
4	2260	71.3	3 540	0.792
5	2300	73.1	2 090	0.882
6	2160	83.5	140	1.035
7	2220	84.9	100	1.049
8	2290	86.0	80	1.071
9	2350	87.1	70	1.096
10	2420	88.1	60	1.111

down to 0.6 K. The most prominent feature of these results is that $H_{c2}(T)$ hardly changes from sample to sample, although the normal-state resistivity varies by more than two orders of magnitude.

Figure 3 exhibits the results of $H_{c2}(T)$ measured on samples with metal concentrations 88–80%. Here the temperature dependence of the upper critical field changes from that of a dirty bulk superconductor (sample 10) to that of a dirty film, or an isolated grain (sample 6). There is a clear-cut crossover between the clean and dirty behaviors.

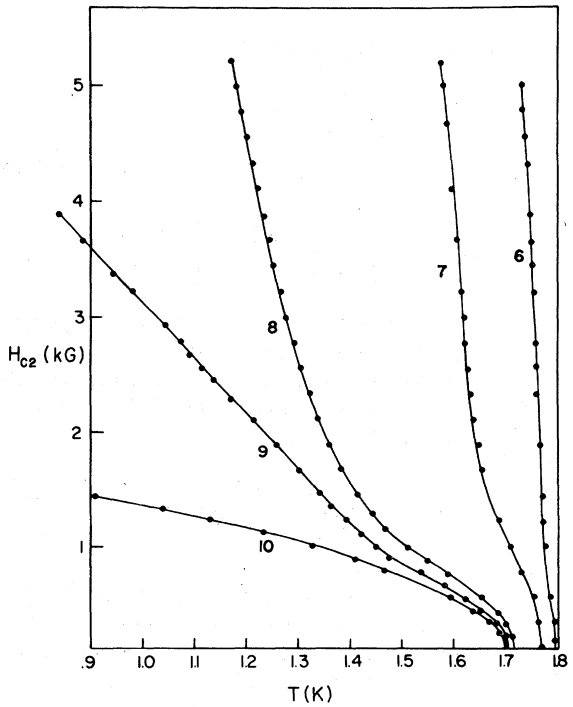

FIG. 3. H_{c2} vs temperature for metal concentrations 80–88% (experimental).

IV. THEORETICAL MODEL

The system studied is a stack of superconducting grains, embedded in a semiconducting or insulating matrix. It is assumed that the grains are coupled together to their nearest neighbors by the Josephson interaction.

The free energy, in the Landau-Ginzburg (LG) context, consists of two parts. The first is the free energy of an isolated grain and the second arises from the coupling of the grain to its nearest neighbors. Here we shall be interested in the LG equation, which reads

$$\alpha\psi_{ij}-\frac{h^2}{2m}\nabla^2\psi_{ij}+\frac{1}{2m}\left[h\vec{\nabla}\phi_{ij}-\frac{2e}{c}A\right]^2\psi_{ij}$$
$$+\eta(-\psi_{i+1j}-\psi_{i-1j}+2\psi_{ij})$$
$$+\eta\{-\psi_{ij+1}\exp[i(2e/hc)HxS]-\psi_{ij-1}$$
$$\times\exp[-i(2e/hc)HxS]+2\psi_{ij}\}=0\ . \quad (1)$$

In writing down Eq. (1), the following notations have been introduced: the external magnetic field $\vec{H}$ is in the y direction and we consider a plane of grains perpendicular to it, in which the vector potential $\vec{A}$ is in the z direction, having the gauge

$$\vec{A}=(0,0,Hx)\ . \quad (2)$$

It should be noted that when H is close to the upper critical field H_{c2}, the order parameter is small. Therefore, the local value of $\vec{A}$ can be taken as the external value, and the cubic term (in the order parameter) in the LG equation is neglected. In Eq. (1), ψ_{ij} and ϕ_{ij}, denote the amplitude and the phase of the order parameter in the ij grain (in the xy

plane), respectively, and α is given by

$$\alpha = -\frac{h^2}{2m\xi^2(T)} = -\frac{\hbar^2}{2m\xi^2(0)}\frac{T_c - T}{T_c} \quad , \tag{3}$$

in which $\xi(T)$ is the coherence length of the isolated grain. The last two terms in Eq. (1) are the coupling terms; η is the coupling energy and S is the "lattice constant" of the stack and is equal to the sum of the grain's diameter $2R$ and the thickness of the junction b. The exponents in the last term arise from the term $i(2e/\hbar c)\int A dz$, which describes the phase difference between two successive grains. The form of Eq. (1) is analogous to the LG equation appearing in the Lawrence-Doniach[8,9] theory for layered superconductors, and to its modification which includes the finite size of the superconducting material.[5] Similar equation was used to analyze H_{c2} of a filamentary superconductor,[10] neglecting the finite size of the filaments.

To simplify Eq. (1), the following approximations are inserted in it: (i) It is assumed that the grain is small enough such that the order parameter across it is almost constant, thus the second term in Eq. (1) may be neglected. (ii) The third term in Eq. (1) (this is the kinetic energy term[11]) can be written as

$$\frac{1}{2m}\left|h\vec{\nabla}\phi_{ij} - \frac{2e}{c}\vec{A}\right|^2 \simeq \frac{h^2}{2m}\left(\frac{2e}{hc}\right)^2 H^2 \tfrac{3}{5} R^2 \psi_{ij} \quad . \tag{4}$$

This results from the fact that in the geometry used here, $h\,\partial\phi_{ij}/\partial z = (2e/cHx)$, and hence $\partial\phi_{ij}/\partial x = (2e/\hbar cHr)$, where r denotes the distance from the grain's center to some point inside the grain; assuming a spherical shape with radius R, we average over the grain's volume, and obtain Eq. (4). (iii) It is assumed that the amplitude of the order parameter varies slowly from grain to grain; therefore, the first coupling term [fourth term in Eq. (1)], may be approximated by

$$\eta(-\psi_{i+1,j} - \psi_{i-1,j} + 2\psi_{ij}) \simeq -\eta S^2 \frac{\partial^2}{\partial x^2}\psi_{ij} \quad , \tag{5}$$

and the second coupling term [last term in Eq. (1)] is

$$2\eta\psi_{ij}\left(1 - \cos\frac{2e}{hc}HSx\right) \quad . \tag{6}$$

Using Eqs. (3)–(6) in Eq. (1) we obtain the following form for the LG equation

$$-\frac{1}{\xi^2}\psi + \left(\frac{2e}{hc}\right)^2 \tfrac{3}{5} H^2 R^2 \psi - \left(\frac{s}{t}\right)^2 \frac{\partial^2\psi}{\partial x^2} + \frac{2}{t^2}\left(1 - \cos\frac{2e}{\hbar c}HxS\right)\psi = 0 \quad , \tag{7}$$

in which we have introduced a "coupling length" t by

$$t^2 = \frac{h^2}{2m\eta} \quad . \tag{8}$$

Equation (7) is similar to the one used by Turkevich and Klemm[10] [Eq. (32) in their paper] to investigate the upper critical field of a filamentary superconductor, when the field is applied parallel to the filaments. This is not surprising, as in this geometry the filamentary stack resembles the granular superconductor. However, we did take into account the finite size of the superconducting material [second term in Eq. (7)], thus we avoid the unphysical divergence of H_{c2} found in Ref. 10.

Introducing the transformation

$$\frac{e}{\hbar c}HSx = \theta, \quad \psi(x) = f(\theta) \quad , \tag{9}$$

Eq. (7) is cast into the form of a Mathieu equation,[12] the lowest eigenvalue of it giving the expression[9–11] for H_{c2}. This can be easily found in two extreme limits:

A. Strong field

When the inequality

$$\frac{S^2 eH}{\hbar c} \gg 1 \tag{10}$$

holds, the lowest eigenvalue of Eq. (7) is given by the expansion[12]

$$a = -\tfrac{1}{2}q^2 + \tfrac{7}{128}q^4 - \tfrac{29}{2304}q^6 + \cdots \quad , \tag{11}$$

in which

$$q = -\left(\frac{\hbar c}{eHS^2}\right)^2 \quad , \tag{12}$$

$$a = \left(\frac{t}{\xi}\frac{\hbar c}{S^2 eH}\right)^2 - \frac{3}{5}\left(\frac{2tR}{S^2}\right)^2 - 2\left(\frac{\hbar c}{S^2 eH}\right)^2 \quad . \tag{13}$$

Equation (11) was solved on the computer, to extract $H \equiv H_{c2}$ as a function of temperature [the temperature dependence appears in ξ, Eq. (3)]. Keeping only the first term on the right-hand side of (11), we obtain, to leading order,

$$H^2 = \left(\frac{\hbar c}{2e}\right)^2 \frac{5}{3}\frac{1}{\xi^2 R^2}\left(1 - 2\frac{\xi^2}{t^2}\right) \quad . \tag{14}$$

When the coupling length t is much longer than the coherence length (i.e., extreme weak-coupling limit), Eq. (14) gives just the upper critical field of a small spherical superconductor of radius R.[13] This results from the kinetic energy term in the LG equation, and has a characteristic $(T_c - T)^{1/2}$ dependence. As the coupling becomes stronger and t is shortened, H_{c2} decreases from the value of an isolated grain.

B. Weak field

When the inequality

$$\frac{S^2eH}{\hbar c} << 1 \tag{15}$$

holds, the lowest eigenvalue of Eq. (7) is given by the expansion[12]

$$a = -2|q| + 2|q|^{1/2} - \tfrac{1}{4} + O(|q|^{-1/2}) \ . \tag{16}$$

Again, the full solution was carried out on the computer. The leading orders are

$$H = \frac{\hbar c}{2e}\left(\frac{t}{S\xi}\right)^2\left\{1 + \frac{1}{4}\left(\frac{t}{\xi}\right)^2\left[\frac{1}{4} - \frac{3}{5}\left(\frac{2tR}{S^2}\right)^2\right]\right\} \ . \tag{17}$$

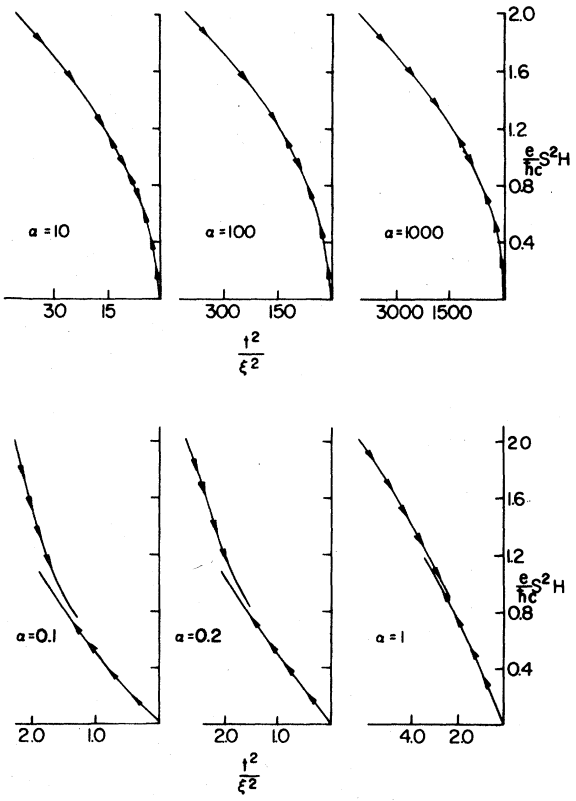

FIG. 4. Calculated curves of $(e/\hbar c)S^2H$ as a function of t^2/ξ^2 (proportional to $T_c - T$) for different values of $\alpha = \frac{3}{5}(2tR/S^2)$ the coupling strength (see text). The downward arrows indicate a solution for strong fields, $(e/\hbar c)S^2H >> 1$, while the upwards arrows indicate the solution for weak fields $(e/\hbar c)S^2H << 1$.

When the second term in the square brackets is small compared to unity, the result resembles H_{c2} of a bulk superconductor, with the same temperature dependence $\sim T_c - T$, but with an effective coherence length $S\xi/t$. When the second term cannot be neglected, it may cause a negative curvature in H_{c2} vs T, which was observed experimentally.[3] In general, depending on the value of $S^2eH/\hbar c$, the upper critical field as a function of temperature may have an upturn point, where the temperature dependence is changed from that of $T_c - T$ to that of $(T_c - T)^{1/2}$.

The calculated curves in Fig. 4 were obtained by computing Eqs. (11) and (16). The figures show $(e/\hbar c)S^2H$ vs $t^2/\xi^2 \sim T_c - T$, for different values of $\frac{3}{5}(2tR/S^2)^2$. Since R and S are almost constant, this means that the plots in Fig. 4 are for different values of the coupling strength. In each curve we have indicated the crossover between the regions of validity of the two approximations. The comparison between these curves and the experimental data is discussed in the next section.

V. DISCUSSION

To compare the model's results with the experimental data, we must express the coupling energy η (or t) in terms of measurable quantities. This is accomplished by equating the usual expression for the Josephson energy[14]

$$\frac{1}{2R_n}\frac{\hbar}{e^2}\frac{1}{8}\pi\frac{\Delta^2(T)}{k_BT_c} \ ,$$

with the expression resulting from the LG free energy, $2\eta\Omega\psi^2$. Here R_η is the normal state resistance of the junction, $\Delta(T)$ is the order parameter (in energy units), and Ω is a typical volume of one unit cell of the grain's lattice. The relation between $\Delta^2(T)$ and ψ^2 is given by[15]

$$\psi^2 = \tfrac{7}{8}\zeta(3)\frac{\Delta^2(T)}{(\pi k_BT_c)^2}\chi N \ , \tag{18}$$

in which $\zeta(3)$ is the Riemann ζ function, N is the electron concentration in the metal, and χ is a function describing the "dirtiness" of the system.[15] In the dirty limit, in which we are interested here,

$$\chi \simeq \frac{2\pi^3}{7\zeta(3)}\frac{k_BT_c}{\hbar}\tau \ ,$$

where τ is the mean free time of the electrons collisions with impurities. Using the free-electron gas definition of the conductivity σ, namely $\sigma = Ne^2\tau/m$, we obtain [see Eq. (8)],

$$\frac{1}{t^2} = \frac{1}{4\Omega}\frac{1}{R_n\sigma} \ . \tag{19}$$

Introducing[16] $R_n = \rho_n/S$ where ρ_n is the normal-state

resistivity and $\Omega = S^3$, we finally get

$$\frac{1}{t^2} = \frac{1}{4S^2\sigma\rho_n} \quad . \tag{20}$$

It should be noted that σ refers to the corresponding value of the bulk material from which the grains are formed, while ρ_n characterizes mainly the junctions between the grains. The same distinction would be made when considering the coherence length $\xi(T)$. In the dirty limit, and at the vicinity of T_c (a situation pertains to H close to H_{c2}), it is given by[1,2,4,5]

$$\xi(T) = 0.85\left(\xi_0 l \frac{T_c}{T_c - T}\right)^{1/2} \quad , \tag{21}$$

where l is the electronic mean free path. Since $\xi(T)$ characterizes the grain, we put $l \sim R$ and evaluate ξ_0 by multiplying[17] the corresponding value of pure Al, 16 000 Å, by the ratio of T_c of pure Al to the T_c of the granular system (of the order $\frac{2}{3}$). From the relation $\xi^2 \sim R$ and Eq. (14), it is seen that when H_{c2} approaches the isolated grain limit, $H \propto R^{-3/2}$. Since R varies slowly with metal concentration, it follows that $H_{c2}(T)$ also changes slowly with metal concentration. This behavior is exhibited in Fig. 2. There, $H_{c2}(T)$ is almost unchanged although the normal-state resistivity changes by two orders of magnitude. Using the experimental value $H = 5$ kG for $(T_c - T)/T_c = 0.1$, pertaining in the isolated grain limit, we find from Eqs. (14) and (21) that $R \sim 45$ Å. This value is quite close to the one deduced from electron microscopy, $R = 50$ Å .

The same qualitative behavior was observed in Al-Al_2O_3 specimens,[3,4] for $\rho_n \geq 3000$ $\mu\Omega$ cm. (Although for these samples the critical field was probably that of the paramagnetic limit.) Note also that $H_{c2}(T)$ in Al-Al_2O_3 samples[3] is approximately three times greater than the values in Fig. 2, a fact explained by the smaller grain radius[6] in Al-Al_2O_3. The upper critical field was calculated in two limiting cases, according to the value of $S^2eH/\hbar c$ compared to unity. The crossover between the two solutions will thus occur for $S^2eH/\hbar c$ of the order 1 and from the computer plots (Fig. 4) we find this point to be $S^2eH/hc \sim 0.8$. Here the experimental result for H is 1–2 kG (Fig. 3) and therefore, we get $S \sim 600$ Å. This is greater than the expected value of $2R + b$. But it should be noted that the relation $S^2eH/hc \sim 1$ at the crossover point goes in the right direction. In the Al-Al_2O_3 specimens of Deutscher and Dodds,[3] where the same upturn was observed, $H \sim 5$ kG and thus S becomes smaller, which is consistent with the smaller grain size in Al-Al_2O_3 samples.

The temperature at which the crossover occurs can be derived from the calculated curves as follows. Let us denote this temperature by T_t and the crossover point on the x axis of Fig. 4 by X_t. Then, since the x axis is t^2/ξ^2 we find

$$X_t = \frac{4\sigma\rho_n S^2}{0.72\xi_0 l T_c}(T_c - T_t) \quad . \tag{22}$$

From Fig. 4 it is seen that $X_t \sim 1.5$ and hence

$$\frac{\sigma}{l}\rho_n S^2 \frac{T_c - T_t}{T_c} \sim \text{const} \quad .$$

Note that both σ and l are parameters of the Al grain and change slowly from sample to sample since S also changes very slowly we get $\rho_n(T_c - T_t)/T_t \simeq$ const. This is indeed observed, as can be verified from Fig. 3 and Table I, within the limits of experimental error. To extract S from Eq. (22) we need to know l/σ and since it is typical of the grain we shall use values observed for bulk Al. Skin effect measurements[18] yield $l/\sigma = 0.4 \times 10^{-11}\,\Omega$ cm^2 while the value derived from resistivity measurements is[19] $l/\sigma = 0.8 \times 10^{-11}\,\Omega$ cm^2. Using the last value we get $S = 700$ Å, again larger than $2R + b$, but similar to the former value. The quantity S can be calculated in another way, as follows: From the experimental data in Fig. 3 it is seen that a crossover point occurs in samples for which $\rho_n \lesssim 100$ $\mu\Omega$ cm. The computer analysis reveals that a crossover takes place for $\frac{3}{5}(2RT/S^2)^2 \lesssim 0.5$. Using $\rho_n = 100$ $\mu\Omega$ cm, $t^2 = 4S^2\sigma\rho_n$, and $R = 75$ Å we find that $S \sim 600$ Å , consistent with the former values, but much higher than $2R + b$.

The reasons for these high values of S (the period of the grain's lattice) are not yet clear to us. Two possible explanations can be offered, both suggest that at $H = H_{c2}$ the grains form clusters, and one should consider the cluster's lattice rather than the grain's lattice. The first explanation is that S is a certain characteristic length which involves the field penetration depth into the Josephson junction. In an isolated junction, this depth is twice the penetration depth into the superconductor, and is of the order 1000 Å. In our case the junctions are not isolated but it may be that S is comparable with the penetration depth. The other explanation is that at the critical field, superconductivity is established by a percolation process. Thus, at H_{c2} we are dealing with clusters, for which the typical length may be greater than R.

We now turn to the strong-coupling limit (small t) of the weak-field case. Two main features are seen from Eq. (17). The first is that in the extreme limit we obtain an expression similar to that of a dirty bulk superconductor,

$$H_{c2}(T) = \frac{hc}{2e}\left(\frac{t}{\xi S}\right)^2 \quad , \tag{23}$$

but with an effective coherence length given by $\xi S/t$. The second is that for $\frac{3}{5}[(2tR)^2/S^2] \leq 0.25$, there is a negative curvature in the magnetic field as a func-

tion of temperature. Such behavior was observed in H_{c2} measurements taken for fields perpendicular to an Al-Al_2O_3 film.[3] For fields parallel to the film plane (of Al-Al_2O_3), the negative curvature is obscured by the $(T_c - T)^{1/2}$ behavior, pertaining to cases in which the film's thickness d is much smaller than the coherence length.[20] We can put these arguments in a semiquantitative way as follows: For an homogenous material, the upper critical field parallel to the surface of a thin slab, of thickness d, is

$$H_{c2}''(T) = \frac{\hbar c}{2e}\frac{\sqrt{12}}{d\xi} \quad . \tag{24}$$

In a granular material the coherence length is modified; we therefore, speculate that the upper critical field parallel to a thin granular film will be

$$H_{c2}''(T) = \frac{\hbar c}{2e}\frac{\sqrt{12}}{d\xi}\frac{t}{S} \quad . \tag{25}$$

Using here Eq. (21) and [from Eq. (20)] $t^2 = 4S^2\sigma\rho_n$, we find that

$$H_{c2}'' = \frac{\hbar c}{2e}\frac{\sqrt{12}2\rho_n^{1/2}}{0.85\xi_0^{1/2}d}\left(\frac{\sigma}{l}\right)^{1/2}\left(\frac{T_c - T}{T_c}\right)^{1/2} \quad . \tag{26}$$

Apart from a factor of 2 this is identical to the expression for H_{c2}'' in a dirty film. Our data for weak fields, taken on samples 7–10 (see Fig. 3), were compared with Eq. (26), and it was found that it is best fitted with $l/\sigma = 2.25 \times 10^{-11}$ Ω cm^2. Other data for critical fields[21] were best fitted by $l/\sigma = 1.2 \times 10^{-11}$ Ω cm^2. In view of the simplified assumptions involved in our model, this is not a serious discrepancy. Also note that we have put [Eq. (20)] $t^2 = 4\sigma\rho_n S^2$ but probably this relation is oversimplified and it is plausible to assume that $t^2 = \delta\sigma\rho_n S^2$, where δ is a constant of order unity. Then, in order to use for l/σ the value extracted from resistivity measurements (0.8×10^{-11} Ω cm^2), we need $\delta = 1.4$.

We have found that our model fits rather well the experimental data at high and intermediate values of metal concentration. At low concentrations (the isolated grain limit), the model yields the measured value of H_{c2} without any adjustable parameter. At first sight, it seems surprising that by an electrical measurement one may observe the critical field of an isolated grain. The answer to this is that the order of magnitude of t^2 required to observe the critical field of the isolated grain is much smaller than the one needed to quench the Josephson coupling. The order of magnitude of t^2 for the (magnetic) isolated grain limit is given from Eqs. (14), (20), and (21). For a supercurrent to flow, the Josephson energy must be at least of the order[22] of $k_B T$. We have found that in the extreme weak-coupling case, where $\rho_n \sim 4 \times 10^4$ $\mu\Omega$ cm, the Josephson energy [see Eq. (18) and discussion before] is still of the order of $k_B T$. Therefore in the range $2 \times 10^2 < \rho_n < 4 \times 10^4$ $\mu\Omega$ cm the weak-coupling limit is reached while the samples are still superconducting.

ACKNOWLEDGMENTS

Research supported by the Israeli Council for Research and Development and by the Karlsruhe Research Center.

[1]B.Abeles, R. W. Cohen, and W. R. Stowell, Phys. Rev. Lett. 18, 902 (1967).
[2]R. W. Cohen and B. Abeles, Phys. Rev. 168, 444 (1968).
[3]G. Deutscher and S. A. Dodds, Phys. Rev. B 16, 3936 (1977).
[4]J. J. Hauser, J. Low Temp. Phys. 7, 335 (1972).
[5]G. Deutscher and O. Entin-Wohlman, Phys. Rev. B 17, 1249 (1978).
[6]G. Deutscher, H. Fenichel, M. Gershenson, E. Grunbaum, and Z. Ovadyahu, J. Low Temp. Phys. 10, 231 (1973).
[7]G. Deutscher, M. Rappaport, and Z. Ovadyahu, Solid State Commun. 28, 493 (1978).
[8]W. Lawrence and S. Doniach, in *Proceedings of 12th International Conference on Low Temperature Physics,* edited by E. Kanda (Academic, Kyoto, Japan, 1971), p. 361.
[9]R. A. Klemm, A. Luther, and M. R. Beasley, Phys. Rev. B 12, 877 (1975).
[10]L. A. Turkevich and R. A. Klemm, Phys. Rev. B 19, 2520 (1979).
[11]P. G. de Gennes, *Superconductivity of Metals and Alloys* (Benjamin, New York, 1966).
[12]N. W. McLachlan, *Theory and Applications of Mathieu Functions* (Dover, New York, 1964).
[13]P. G. de Gennes and M. Tinkham, Physics (N.Y.) 1, 107 (1964).
[14]B. D. Josephson, in *Superconductivity,* edited by R. D. Parks (Marcel Dekker, New York, 1969).
[15]N. R. Werthamer, in *Superconductivity,* edited by R. D. Parks (Marcel Dekker, New York, 1969).
[16]B. Abeles, R. W. Cohen, and G. W. Cullen, Phys. Rev. Lett. 17, 632 (1966).
[17]Ref. 5, p. 24.
[18]E. Fawcett, in *The Fermi Surface,* edited by W. A Harrison and M. B. Webb (Wiley, New York, 1961), p. 197.
[19]I. Holwech and J. Jeppeson, Philos. Mag. 15, 217 (1967).
[20]D. Saint-James and P. G. de Gennes, Phys. Lett. 7, 306 (1963).
[21]B. Abeles, in *Applied Solid State Science,* edited by R. Wolfe (Academic, New York, 1976), Vol. 6, p. 1.
[22]L. Solymer, *Superconducting Tunneling and Applications* (Chapman and Hall, London, 1972).